

ISFA2012-7% %

ROBUST CONTROL DESIGN OF A SINGLE DEGREE-OF-FREEDOM MAGNETIC LEVITATION SYSTEM BY QUANTITATIVE FEEDBACK THEORY

Feng Tian

Department of Mechanical Engineering
Marquette University
Milwaukee, WI 53233
Email: feng.tian@marquette.edu

Mark Nagurka

Department of Mechanical Engineering
Marquette University
Milwaukee, WI 53233
Email: mark.nagurka@marquette.edu

ABSTRACT

A magnetic levitation (maglev) system is inherently nonlinear and open-loop unstable because of the nature of magnetic force. Most controllers for maglev systems are designed based on a nominal linearized model. System variations and uncertainties are not accommodated. The controllers are generally designed to satisfy gain and phase margin specifications, which may not guarantee a bound on the sensitivity. To address these issues, this paper proposes a robust control design method based on Quantitative Feedback Theory (QFT) applied to a single degree-of-freedom (DOF) maglev system. The controller is designed to successfully meet the stability requirement, robustness specifications, and bounds on the sensitivity. Experiments verify that the controller maintains stable levitation even with 100% load variation. Experiments prove that it guarantees the transient response design requirements even with 100% load change and 39% model uncertainties. The QFT control design method discussed in this paper can be applied to other open-loop unstable systems as well as systems with large uncertainties and variations to improve system robustness.

I. INTRODUCTION

Magnetic levitation (maglev) technology is used in high-speed transportation systems, frictionless bearing systems, vibration isolation systems, and photolithography systems [1]. Systems using maglev technology have many advantages over their counterparts using traditional mechanical parts. In high-speed maglev train systems and magnetic bearing systems, non-contact

electromagnetic forces are utilized to constrain the motions of the moving components. There is no physical contact between dynamic and static components, and therefore no friction, abrasion, or noise [2–5]. In vibration isolation systems, electromagnetic forces can be tuned according to the displacements of the positioning stages, providing a controllable non-contact stiffness [6]. Maglev technology is also utilized to improve the accuracy of fine motion control systems. In photolithography, it allows for a relatively large motion range at low cost, in comparison to the conventional mechanical actuators [7].

Although maglev systems are seen in many applications, their controllers are not designed to deal with large system variations. Conventional control design methods usually involve linearizing system nonlinearities and then designing controllers for the linearized model [8–12]. Maglev systems are able to achieve levitation with controllers designed using these approaches, but they require the levitated objects to stay in the vicinity of the linearized point. If the systems experience parameter changes, the unmodeled nonlinearities drive the systems away from the linearized point, and eventually the systems become unstable. In reality, system parameter changes are common. Two examples of changes in the levitated load are: (1) a magnetic bearing experiences a working load change on the rotor during operation, and (2) a maglev train has different load conditions as the number of passengers varies.

The challenge of dealing with system parameter changes can be solved by improving the system robustness. Many robust controllers have been proposed. Yang et al. [13] reported a backstepping design method for a nonlinear controller. In their research,

a disturbance observer was introduced to suppress the uncertainties. A high-gain observer was also included to estimate the immeasurable state of the system. Vagia [14] reported a robust PID controller coupled with a feedforward compensator. In this research, the system was linearized at multiple operating points, and the feedforward compensator was utilized to provide nominal bias voltage, and the PID controller had multiple gains associated with multiple operating points. Shan [15] presented two disturbance rejection algorithms to improve the dynamic stiffness of a magnetic-suspension stage. This study suggested using an internal model principle-based control together with a frequency estimator based on adaptive-notch filtering to reject narrow-band disturbances with unknown frequencies. Satoh et al. [16] proposed a control Lyapunov function based robust nonlinear adaptive controller. Their controller consisted of a pre-feedback compensator with an adaptive control mechanism and a robust stabilizing controller. In his doctoral dissertation, Green [17] studied adaptive backstepping control (ABC) and feedback linearization control (FLC) for a single DOF maglev system. Green concluded that ABC control was superior to FLC in terms of system robustness. The above-mentioned researchers all focused on designing systems to meet the classical measurement of robustness, i.e., gain and phase margin. However, as Yaniv and Nagurka [18] discussed, although a controller can be designed to meet the gain and phase margin specifications, it might fail to guarantee a reasonable bound on the sensitivity.

To address robustness issues and guarantee bounds on sensitivity, this paper presents a control design approach with Quantitative Feedback Theory (QFT) for maglev systems. QFT is a robust control design method introduced by Horowitz [19]. It has the unique characteristics of designing controllers for systems with large changes (due to parameter variations or model uncertainties) that satisfy gain margin specifications and bounds on the sensitivity. In this study, a PID type controller is developed using QFT. Yaniv and Nagurka [18] proved that PID type controllers can be designed to guarantee gain and phase margin specifications and sensitivity constraints for a set of plants. This research models a single DOF maglev system with large parameter changes as a set of plants, and demonstrates the control design process following the steps proposed by Yaniv [20]. Experiments are conducted to verify that the QFT controller meets the design goals.

The paper is organized as follows. Section II presents the system model of the maglev system and the control design goals. In Section III a single DOF controller is designed for the maglev system to meet the design requirements following the procedure suggested by Yaniv [20]. Section IV describes the experimental tests and results. Section V presents the conclusions.

II. Single DOF Maglev System Model and Control Design Goals

The single DOF maglev device used in this research, shown in Fig. 1, consists of an electromagnet bolted to an aluminum frame. When a current passes through the electromagnet, the electromagnetic force will pull a ferrous object (in this case, a steel ball) up. An infrared emitter and detector pair is used to measure the gap distance between the ball and the electromagnet.

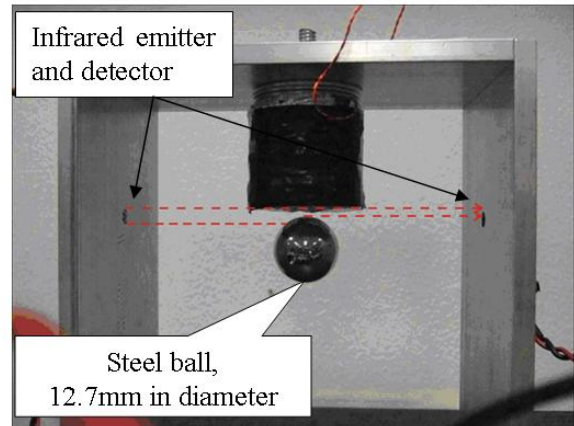


FIGURE 1. MAGLEV APPARATUS

A controller is needed to control the magnitude of the electromagnetic force according to the gap distance to counterbalance gravity and levitate the ball. The electromagnetic force is used to manipulate the vertical position of the ball. The system is viewed as a single DOF system. Other DOF's of the ball are neglected in this research.

Fig. 2 shows a schematic of the electromagnet and the ball, where V is the voltage across the electromagnet; i is the current passing through the electromagnet; R and L are the resistance and inductance of the electromagnet, respectively; m is the mass of the ball; x is the gap distance between the electromagnet and the ball; F is the electromagnetic force acting on the ball.

The magnitude of the attractive force F between the electromagnet and the ball has been modeled by Woodson and Melcher [21] as a function of current i and gap distance x :

$$F(i, x) \cong K_1 \left(\frac{i}{K_2 + x} \right)^2 \quad (1)$$

where constants K_1 and K_2 are force and distance constants, respectively, characterized by the geometry of the electromagnet and construction of the apparatus, and determined experimentally.

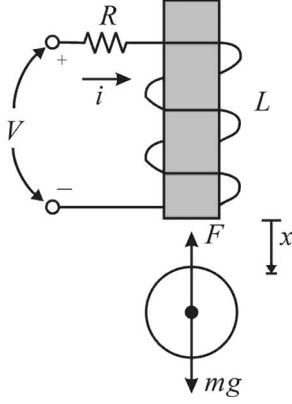


FIGURE 2. SCHEMATIC OF ELECTROMAGNET AND BALL

Given the function of the electromagnetic force in Eqn. (1), the open loop transfer function of the maglev system can be calculated, as shown in [22]. The transfer function between the input (the control current) and the output (the gap distance) is:

$$\frac{X(s)}{I(s)} = \frac{-k_i}{s^2 - k_x} \quad (2)$$

where k_i and k_x are parameters determined by the current and gap distance at the linearized point. The transfer function has a pair of real poles at $\pm\sqrt{k_x}$, as is shown in Eqn. (2). The plant is open loop unstable because of the positive real pole. The first design goal of the controller is to compensate the positive real pole and enable the maglev system to achieve a stable levitation.

The values of the system parameters, k_i , k_x , K_1 , and K_2 , are measured experimentally in this research. Table 1 shows the values of the model parameters and uncertainties measured at one linearized point ($x_0 = (5.3 \pm 0.2) \times 10^{-3}$ m and $i_0 = (0.289 \pm 0.0005)$ A).

In control designs reported previously in the literature, k_i and k_x are assumed to be constants. This assumption is incorrect if either the gap distance or the levitated loading is changed. To demonstrate the variation of the values of k_i and k_x , an 8.3 g ball is levitated, then the gap distance is changed from $x_0 = 1.35$ mm to $x_0 = 5.00$ mm, and k_i and k_x are experimentally measured. It is found that the values of k_i and k_x vary within two sets of values.

$$k_i \in [4.72 \times 10^{-1}, 7.37 \times 10^{-1}] \quad (3)$$

and

$$k_x \in [39.1, 79.4] \quad (4)$$

If the maglev system is designed to operate at a gap distance $x_0 = 3.8$ mm, the measured values are $k_i = 5.91 \times 10^{-1}$ m/A-s²

TABLE 1. MODEL PARAMETERS AND VALUES

Model Parameter	Measured Values	Unit
m	$(8.3 \pm 0.05) \times 10^{-3}$	kg
x_0	$(5.3 \pm 0.2) \times 10^{-3}$	m
R	31.08 ± 0.005	Ω
i_0	0.289 ± 0.0005	A
K_1	1.08 ± 10^{-5}	$\frac{\text{N}\cdot\text{s}^2}{\text{A}^2}$
K_2	8.86 ± 10^{-6}	m
k_x	3270	$\frac{\text{m}}{\text{s}^3}$
k_i	67.89	$\frac{\text{m}}{\text{A}\cdot\text{s}^2}$

and $k_x = 64.2$ m/s³. Compared to the values in Eqns. (3) and (4), it is found that the value of k_i has 24.7% uncertainty and the value of k_x has 39.1% uncertainty. Additionally, when k_i and k_x are derived as done in [22], the levitated mass m was assumed to be a constant. Since both k_i and k_x have m in their expressions, the uncertainties associated with their values will change if m varies. The second design goal of the controller is to accommodate the uncertainties and variations in the plant. In summary, the designed controller should guarantee: (1) stability, which means the maglev system is able to levitate the ball, and (2) robustness, which means the maglev system is able to deal with the model uncertainties and load change (in this case, any change in the levitated mass m).

III. QFT Control Design

This section details the design of a QFT controller for the maglev system plant found in Section II, shown in Eqn. (2). The parameter variations are shown in Eqns. (3) and (4). The nominal plant is chosen as the model found when gap distance $x_0 = 3.8$ mm (where $k_i = 5.91 \times 10^{-1}$ m/A-s² and $k_x = 64.2$ m/s³), without any uncertainties included. The system performance specifications are chosen as suggested in references [17,23]. For this research, the chosen stability margins and tracking specifications are listed below.

1. Stability margins: Gain margin ≥ 5.5 dB, phase margin ≥ 45 deg.
2. Tracking specifications: 90% rise time $t_r \in [0.1, 0.5]$ s, overshooting $M_p \leq 15\%$, and steady state error $e_{ss} \leq 5\%$.

To begin the QFT control design, the templates for the control plant must be calculated. Templates, as stated in reference [20], are

...the sets of all complex numbers for a given set of transfer functions, evaluated at a given frequency...

Reflected on the plot, the plant templates were determined by plotting the frequency response of every possible combination of the uncertain parameter values and then finding the boundaries of these responses. The templates are built with the plants that cover the range of parameter uncertainties. As suggested in [17] this maglev system was designed to operate at control signal frequencies less than 15 Hz. However, research on the apparatus found that the infrared sensor noise had a natural frequency of 22 Hz [22]. To avoid resonance of the sensor's noise, the highest control signal frequency was limited to 10 Hz, which is 62.8 rad/s. Five frequencies are used in this design: $\omega = 0.1, 0.5, 3, 15, 60$ rad/s. The templates obtained at these frequencies are plotted in Fig. 3.

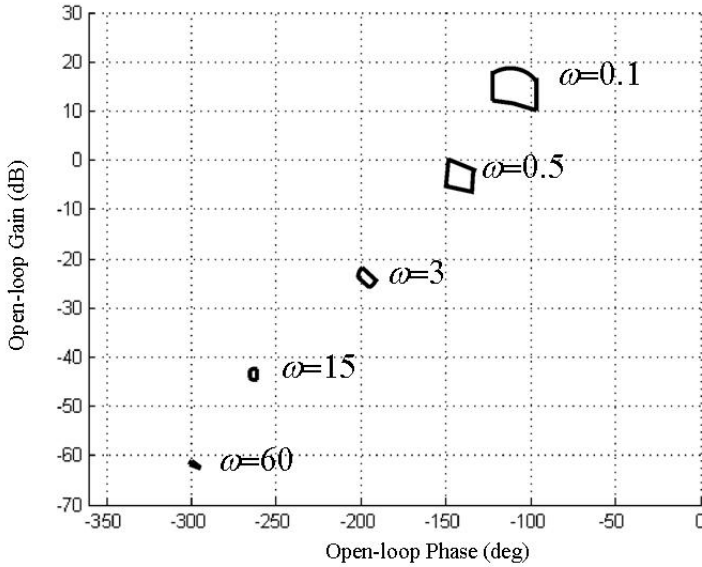


FIGURE 3. MAGLEV SYSTEM PLANT TEMPLATES

The model uncertainties have been accommodated by the plant templates. The next step is to design for the command following ability, or “tracking” of the system. It guarantees the system responses to the command signal be the same despite the system changes (such as changes in the operating point). The tracking models are determined using specifications discussed at the beginning of this section, with 90% rise time between 0.1 and 0.5 s and overshoot less than 20%. Using these criteria, the transfer function for the upper bound T_U and lower bound T_L are calculated to be:

$$T_U = \frac{0.6944}{s^2 + 0.7599s + 0.6944} \quad (5)$$

and

$$T_L = \frac{1.25}{s^2 + s + 0.25} \quad (6)$$

It is a common approach to reshape bounds to relax the constraints on the higher frequencies. This will help the design of pre-filter since the relaxed constraints allow simpler pre-filter forms. To reshape the bounds, zeros and poles are placed into the upper bound and the lower bound transfer functions, respectively. The reshaping process has no influence on the response curve, only shifting the upper and lower bounds on the Bode magnitude plot. Fig. 4 shows the Bode magnitude plot for the original model bounds and the “reshaped” model bounds.

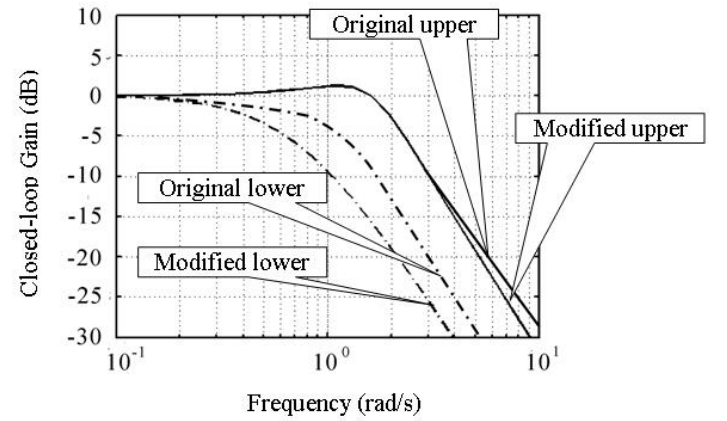


FIGURE 4. BODE MAGNITUDE PLOT OF BOUNDS

The stability margin is determined based on the desired gain margin and phase margin for all plants in the set $\{P\}$. As shown in [20] the stability margin can be calculated using Eqns. 7 and 8.

$$GM = 20 \log \left(1 + \frac{1}{SM} \right) \quad (7)$$

and

$$PM = 180 - \cos^{-1} \left(\frac{0.1}{SM^2} - 1 \right) \quad (8)$$

The bounds and stability margins for chosen frequencies are plotted on a Nichols chart for each frequency value using the MATLAB® QFT toolbox, as is shown in Fig. 5.

Using these bounds, the nominal loop transfer function L_0 should pass below and to the right of the oval bounds (stability

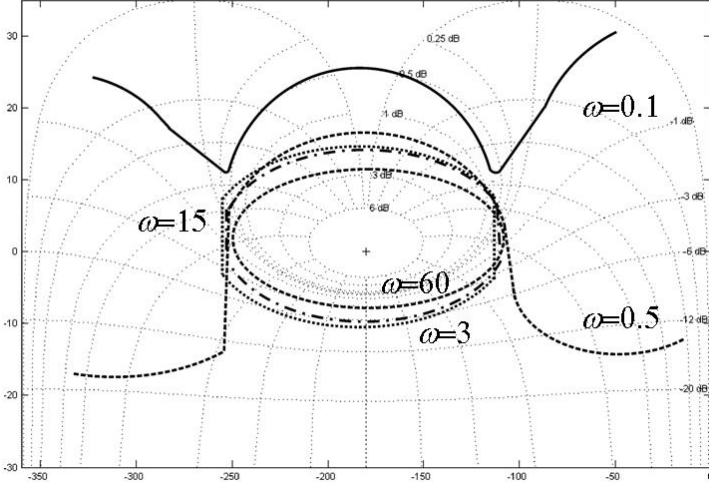


FIGURE 5. BOUNDS ON A NICHOLS CHART

bounds) and should lie above the line bounds (tracking bounds) at the specific frequencies [20]. To meet these requirements, poles and zeros are combined to shift L_0 on the Nichols chart. One controller that ensures that the loop transfer function meets the specifications is found to be:

$$G(s) = \frac{50.33 \left(\frac{s}{7.10} + 1 \right) \left(\frac{s}{18.49} - 1 \right)}{\left(\frac{s}{105.67} + 1 \right)} \quad (9)$$

Controller $G(s)$ in Eqn. (9) guarantees the system steady-state response meets the design specifications. In order to guarantee the transient response of the system also meets the design requirements, a pre-filter should be added to the system. The pre-filter shapes the loop transfer function on the Bode magnitude plot by adding poles and zeros to the system transfer function. Once the response curves are inside the region between the upper and lower bounds, the transient response requirements are met. In this research, the pre-filter is found to be:

$$F(s) = \left(\frac{1}{\frac{s}{50.4} + 1} \right) \left(\frac{\frac{s}{11.91} + 1}{\frac{s}{25.17} + 1} \right) \quad (10)$$

To validate the controller and the pre-filter, the step input response curves of a set of uncertain plants are plotted in Fig. 6. It is shown that the system has already met all the design specifications. Further experimental evaluation of the system is described in Section IV.

IV. Experimental Validation

The evaluation of the performance of the maglev system with a QFT controller includes two experiments. One verifies

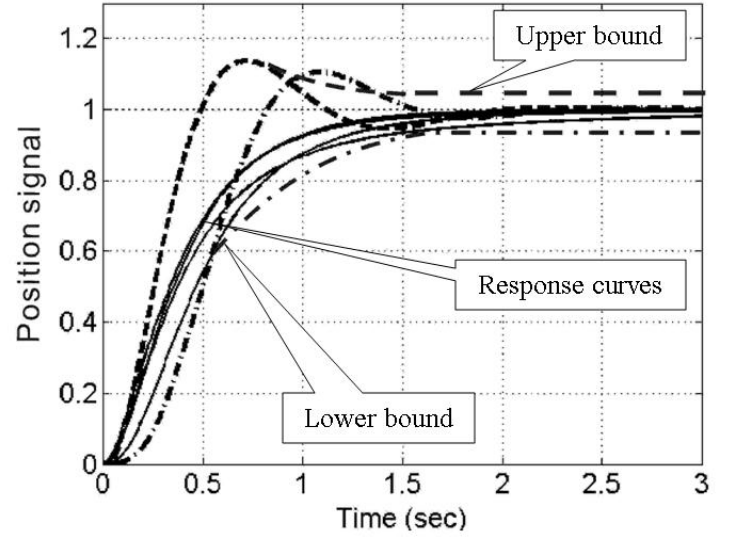


FIGURE 6. CONTROLLER SIMULATION

the stability requirements have been met. In this experiment, a steel ball with a mass of 8.3 g (which is the mass used in the nominal control plant) is steadily levitated. A position change command increases the gap distance by 1 mm at $t = 1$ s. Fig. 7 is the gap distance variation after the position command is issued. It is shown that at $t = 3$ s, the ball reaches steady state at the new position. In other words, the system stability requirement has been met.

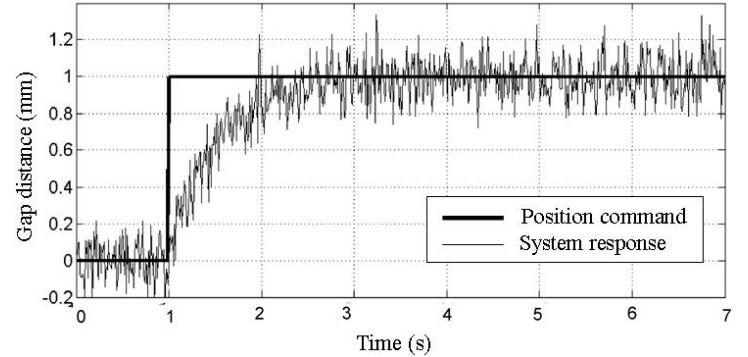


FIGURE 7. STEP RESPONSE OF 8.3 GRAM BALL TRACKING POSITION COMMAND

A second experiment validates that the system has met the designed robust specifications. The levitation load change is tested by using steel balls with different masses. It is desired that the system response will meet all the design specifications despite the load variation and system uncertainties. This experiment uses a step function in the position command to validate

system tracking ability, and the system responses are recorded. Two steel balls, one 8.3 g and the other 16 g, are steadily levitated before the step position change commands. Figs. 8 and 9 show the response curves of cases with the different loads. The response curves show that:

1. Overshoot is increased about 30% in the case where the 16 g mass is levitated;
2. The rise times for the two load cases are about 0.3 s;
3. The settling time for the positions to reach 10% of their final values are about 2.5 s.

Besides the overshoot, the rise time and settling time of the maglev system are almost identical despite the load variations. The second experiment proves the designed QFT controller is robust enough to deal with a variation of almost twice as much as the designed loading. The specifications for the system robustness are successfully met.

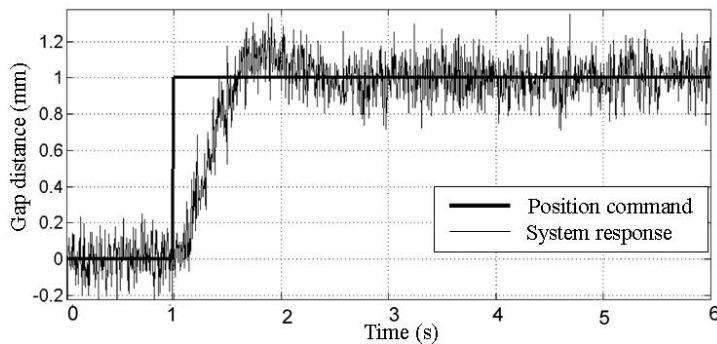


FIGURE 8. STEP RESPONSE OF 8.3 GRAM BALL TRACKING POSITION COMMAND

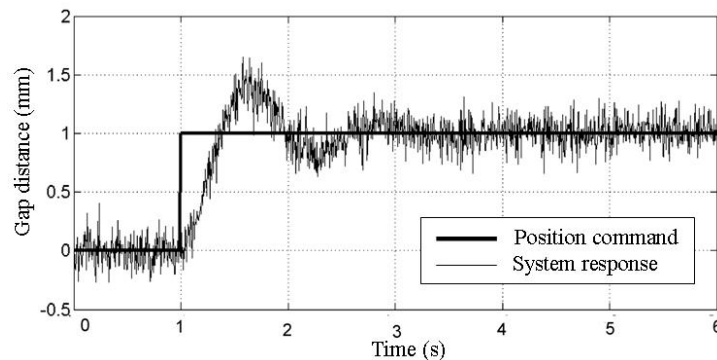


FIGURE 9. STEP RESPONSE OF 16 GRAM BALL TRACKING POSITION COMMAND

V. CONCLUSION

This paper presents a robust control design method based on QFT. Implemented on the single DOF maglev system studied in this research, the QFT controller successfully performs in dealing with a levitation load change up to 100% and accommodates parameter uncertainties up to 39%. The system performance specifications are all met despite the system changes and uncertainties. Based on the results presented in this paper, the QFT controller is able to guarantee stability and robust requirements for maglev system. The same design process can be applied to the other systems to improve system robustness [24].

REFERENCES

- [1] Gotzein, E., Meismger, R., and Miller, L., 1980. "The 'Magnetic Wheel' in the suspension of high-speed ground transportation vehicles". *IEEE Transactions on Vehicular Technology*, **29**(1), February, pp. 17–28.
- [2] Schweitzer, G., and Maslen, E. H., eds., 2009. *Magnetic bearings - theory, design and application to rotating machinery*. Springer-Verlag.
- [3] Shu, G., Meisinger, R., and Shen, G., 2007. "Modeling and simulation of Shanghai maglev train transrapid with random track irregularities". *Sonderdruck Schriftenreihe der Georg-Simon-Ohm-Fachhochschule Nrnberg*, **39**, pp. 3–14.
- [4] Lee, H., Kim, K., and Lee, J., 2006. "Review of maglev train technologies". *IEEE Transactions on Magnetics*, **42**(7), July, pp. 1917–1925.
- [5] Yang, J., Sun, R., Cui, J., and Ding, X., 2004. "Application of composite fuzzy-PID algorithm to suspension system of Maglev Train". *The 30th Annual Conference of the IEEE Industrial Electronics Society*, pp. 2502–2505.
- [6] Eastham, A. R., and Hayes, W. F., 1988. "Maglev systems development status". *IEEE AES Magazine*, **3**, Jan, pp. 21–30.
- [7] Trumper, D. L., 1990. "Magnetic suspension techniques for precision motion control". PhD thesis, Massachusetts Institute of Technology, Cambridge, MA.
- [8] Cicion, J., 1996. "Build a magnetic ball levitator". *Popular Electronics*, May, pp. 48–52.
- [9] Cho, D., Kato, Y., and Spilman, D., 1993. "Sliding mode and classical controllers in magnetic levitation systems". *IEEE Control Systems*, **13**, pp. 42–48.
- [10] Covert, E. E., 1988. "Magnetic suspension and balance systems". *IEEE AES Magazine*, **3**, May, pp. 14–22.
- [11] Carmichael, A. T., Hinchliffe, S., Murgatroyd, P. N., and Williams, I. D., 1986. "Magnetic suspension systems with digital controllers". *Rev. Sci. Instrum.*, **57**(8), pp. 1611–1615.
- [12] Braunbeck, W., 1939. "Free suspension of bodies in elec-

- tric and magnetic fields”. *Zeitschrift für Physik*, **112**(11), pp. 753–763.
- [13] Yang, Z., Hara, S., Kanae, S., and Wada, K., 2011. “Robust output feedback control of a class of nonlinear systems using a disturbance observer”. *IEEE Transaction on Control System Technology*, **19**, March, pp. 256–268.
 - [14] Vagia, M., and Tzes, A., 2008. “Robust PID control design for an electrostatic micromechanical actuator with structured uncertainty”. *IET Control Theory Appl.*, **2**, pp. 365–373.
 - [15] Shan, X., and Menq, C., 2002. “Robust disturbance rejection for improved dynamic stiffness of a magnetic suspension stage”. *IEEE/ASME Transaction on Mechatronics*, **7**, pp. 289–295.
 - [16] Satoh, Y., Nakamura, H., Nakamura, N., Katayama, H., and Nishitani, H., 2009. “Robust adaptive control of nonlinear systems with convex input constraints: Case study on the magnetic levitation system”. *ICROS-SICE International Joint Conference 2009*, pp. 4411–4416.
 - [17] Green, S. A., 1997. “Robust nonlinear control of magnetic-levitation systems”. PhD thesis, Rensselaer Polytechnic Institute, Troy, New York.
 - [18] Yaniv, O., and Nagurka, M., 2005. “Automatic loop shaping of structured controllers satisfying QFT performance”. *Journal of Dynamic Systems, Measurement and Control*, **127**, pp. 472–477.
 - [19] Horowitz, I. M., 1993. *Quantitative Feedback Design Theory (QFT)*. QFT Publications.
 - [20] Yaniv, O., 1999. *Quantitative Feedback Design of Linear and Nonlinear Control Systems*. Springer.
 - [21] Woodson, H. H., and Melcher, J. R., 1968. *Electromechanical Dynamics*. John Wiley & Sons Inc.
 - [22] Tian, F., Craig, K., and Nagurka, M., 2011. “Disturbance attenuation in a magnetic levitation system with acceleration feedback”. *2011 IEEE International Conference on Industrial Technology (ICIT)*.
 - [23] Ogata, K., 2001. *Modern Control Engineering*. Prentice Hall.
 - [24] Mahmoud, N. I., 2003. “A backstepping design of a control system for a magnetic levitation system”. PhD thesis, Linköpings Universitet.